Biochimica et Biophysica Acta 1850 (2015) 287–298

Contents lists available at ScienceDirect

Biochimica et Biophysica Acta

journal homepage: www.elsevier.com/locate/bbagen

Neuroprotection by Kukoamine A against oxidative stress may involve N-methyl-D-aspartate receptors

Xiao-Long Hu [a,b], Ling-Yue Gao [b], Yi-Xuan Niu [b], Xing Tian [b], Jian Wang [b], Wei-Hong Meng [b], Qiao Zhang [b], Can Cui [b], Lu Han [b], Qing-Chun Zhao [a,*]

[a] Department of Pharmacy, General Hospital of Shenyang Military Area Command, Shenyang 110840, China
[b] Department of Traditional Chinese Medicine, Shenyang Pharmaceutical University, Shenyang 110016, China

ARTICLE INFO

Article history:
Received 6 July 2014
Received in revised form 1 November 2014
Accepted 4 November 2014
Available online 8 November 2014

Keywords:
NMDA
Hydrogen peroxide
Molecular docking
Kukoamine A
SH-SY5Y
Neuroprotection

ABSTRACT

Background: Accumulative evidences have indicated that oxidative-stress and over-activation of N-methyl-D-aspartate receptors (NMDARs) are important mechanisms of brain injury. This study investigated the neuroprotection of Kukoamine A (KuA) and its potential mechanisms.
Methods: Molecular docking was used to discover KuA that might have the ability of blocking NMDARs. Furthermore, the MTT assay, the measurement of LDH, SOD and MDA, the flow cytometry for ROS, MMP and Annexin V-PI double staining, the laser confocal microscopy for intracellular Ca^{2+} and western-blot analysis were employed to evaluate the neuroprotection of KuA.
Results: KuA attenuated H_2O_2-induced cell apoptosis, LDH release, ROS production, MDA level, MMP loss, and intracellular Ca^{2+} overload (both induced by H_2O_2 and NMDA), as well as increased the SOD activity. In addition, it could modulate the apoptosis-related proteins (Bax, Bcl-2, p53, procaspase-3 and procaspase-9), the SAPKs (ERK, p38), AKT, CREB, NR2A and NR2B expression.
Conclusions: All the results indicated that KuA has the ability of anti-oxidative stress and this effect may partly via blocking NMDARs in SH-SY5Y cells.
General significance: KuA might have the potential therapeutic interventions for brain injury.

1. Introduction

According to the report of World Health Organization (WHO), stroke will be an important reason of death and disability in the year 2020 and ischemic stroke of which is 67.3% to 80.5% [1]. In the process of ischemic stroke or reperfusion, a large number of ROS are generated and the reactive oxygen species (ROS) could easily attack the membrane that constitutes with high content of polyunsaturated such as neuronal cell membrane and mitochondrial membrane [2–5]. At the same time, ROS can break the balance between oxidants and antioxidants leading to oxidative stress and play a crucial role in brain injury. So how is ROS generated? Accumulative studies have shown that excessive stimulation of NMDARs causes numbers of Ca^{2+} influx and the increased Ca^{2+} leads to oxidative stress which is the main step of ischemic stroke [6–8]. Therefore, the antagonists of NMDAR are considered to be a kind of potential drug for curing ischemic stroke. However, the existing NMDAR antagonists MK-801 cannot protect neurons against oxidative stress bringing about a bad outcome in clinical trials for treatment of ischemic stroke [9,10]. So it is urgent to find a bioactive compound with the anti-oxidative stress ability and the capacity of blocking NMDARs in clinical trials for the treatment of ischemic stroke.

Molecular docking helps in the drug design process and could reduce the number of candidates for experimental validation [11]. Computational methods are the successful tools in the area of drug designing and screening activity auxiliary and could speed up the process of screening potent functional components with the desired biological activity. Complementary to experimental work, molecular docking methods have been used to predict and conjecture the relationship between bioactivity and action mechanism [12]. Discovery Studio (DS) is one of the commonly used docking software for structure based bioactive screening and underlying mechanism prediction [13]. So far thousands of the natural products have been separated and the traditional drug development methods cannot meet the requirements of high-throughput screening. Thus, molecular docking was used in this study to discover a potential bioactive compound from TCM database [14].

Cortex lycii radicis, a traditional Chinese herb, was generally used as a tonic and reported to exhibit hypotensive, hypoglycemic, antipyretic and anti-stress ulcer activity in animal experiment [15,16]. KuA is a major bioactive component in *Cortex lycii radicis* and the chemical structure was shown in Fig. 1. Up to now, the only confirmed

* Corresponding author at: Department of Pharmacy, General Hospital of Shenyang Military Area Command, 83 Wenhua Road, Shenyang 110016, China. Tel./fax: +86 24 28856205.
E-mail address: zhaoqingchun1967@163.com (Q.-C. Zhao).

http://dx.doi.org/10.1016/j.bbagen.2014.11.006
0304-4165/

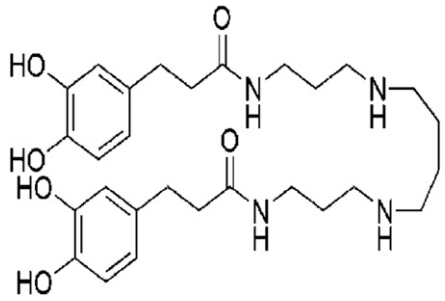

Fig. 1. Chemical structure of Kukoamine A.

pharmacological effect of KuA is the anti-hypertension effect in a rat model [17], but the neuroprotective effects of KuA and its underlying mechanism are unknown.

In our research, NMDARs as a target in molecular docking were used to screen out KuA. H_2O_2-induced cell injury model was used to study the anti-oxidative stress ability of KuA and its potential mechanisms. And simultaneously NMDA-induced Ca^{2+} overload model was used to preliminary verify the blocking capacity of KuA on NMDARs. Then molecular docking was employed to simulate the possible combination between KuA and NMDARs.

2. Materials and methods

2.1. Reagents and antibodies

KuA was purchased from the Chengdu Biopurify Phytochemicals Ltd. (China) with greater than 98.22% purity. Antibodies for p-AKT and t-AKT were purchased from Bioworld Technology (Inc. Minneapolis, USA). Antibodies for p-ERK1/2, t-ERK, p-JNK, t-JNK, p-p38, t-p38, p-CREB, t-CREB, t-NR2A and t-NR2B were purchased from Cell Signaling Technology (Inc. USA). Antibodies for cytochrome c (A-8), Bcl-2 (C21), Bax (P-19), caspase-3, caspase-9, p53 and anti-mouse β-actin (C4) were purchased from Santa Cruz Biotechnology (Santa Cruz, CA). The secondary antibodies were purchased from ZSGB-BIO (Beijing, China). The enhanced chemiluminescent (ECL) plus reagent kit was obtained from the Beyotime Institute of Biotechnology (Nanjing, China). The H_2O_2 was purchased from Sigma (Sigma, USA).

2.2. Computational methods

2.2.1. Virtual screen to find potential NMDAR antagonists

To find new NR2B antagonists, molecular docking was used in this study. X-ray crystal structure of NMDARs (PDB ID:3QEL) was obtained from the Protein Data Bank (PDB) (http://www.wwpdb.org). The SYBYL 6.9.1 software was used to prepare the protein required in docking. Ligands and water molecules were removed from the crystal structures of the protein, and hydrogen atoms were added. Charges were assigned to the atoms according to the method of AMBER7FF99. A short minimization (100 steepest descent steps with Tripos force field) was performed to release internal strain. At our screening, LibDock/DS (Discovery Studio 3.0) module was used to screen more than 30,000 compounds from a Traditional Chinese Medicine (TCM) database, all the compounds were docked into the active site of NMDARs to identify ligands which geometrically fit within the active site.

2.2.2. Analysis of the relationship between NMDARs and KuA

Complex/DS module was used to analyze the geometric binding pattern and the energy binding pattern. NMDARs were defined as the receptor and KuA as the ligand. The active-pocket of NMDARs is located in NR2B subunit. A 2D diagram of their interaction is manifested to confirm, and their docking pose was presented for the analysis of the interactions, including hydrogen bond, hydrophobic bond, π–π interaction and so on.

2.3. Cell culture

Human neuroblastoma SH-SY5Y cells were cultured in DMEM-F12 (1:1) medium supplemented with 10% FBS. Cells were incubated at 37 °C in a humidified atmosphere incubator of 5% CO_2. The culture medium was changed every other day and the cells were subcultured once they reached 70–80% confluence. SH-SY5Y cells were seeded in different kinds of culture dish for 24 h and pretreated with different concentrations of KuA (final concentrations: 5, 10, 20 μM) for 12 h, then added H_2O_2 (final concentrations: 600 μM) for 3 h. After these treatments, the supernatant or the cells were used for the subsequent experiments.

2.4. Cell viability assay

MTT assay was used to determine the protective effect of KuA on cell survival. The cells were cultured in 96-well plates (1×10^5 cells/ml), at the end of indicated treatments, the medium was replaced with fresh medium containing MTT (0.5 mg/ml) incubated for 4 h at 37 °C and the formed insoluble formazan crystals were dissolved by addition of 150 μl DMSO, the absorbance at 490 nm was measured by a microplate reader (Elx800 Bio-Tek, USA).

2.5. Lactate dehydrogenase (LDH) release

The cytotoxicity of H_2O_2 and the protective effect of KuA were further evaluated by LDH assay, which was based on the principle that the leakage of cytosolic LDH increased as the number of dead cells increases. The cells were cultured in 96-well plates (1×10^5 cells/ml) and at the end of indicated treatments, the supernatant was collected to detect the LDH release according to the manufacturer's instructions. The LDH release was quantified by measuring absorbance at 450 nm with a microplate reader (Elx800 Bio-Tek, USA).

2.6. Hoechst 33342 staining

SH-SY5Y cells were seeded into 6-well plates (2×105 cells/well) the cells were treated as described earlier. After these treatments, the cells were washed with PBS solution and loaded with 10 μg/ml Hoechst 33342 dye for 15 min in the dark. Then the cells were visualized under a fluorescence microscope (IX71, Olympus, Japan) and cell images were recorded.

2.7. Annexin V-FITC and propidium iodide (PI) double staining assay

Early apoptosis and necrosis were identified by means of double fluorescence staining with Annexin V and PI. It was dyed by a commercially available kit (BD Pharmingen, CA, USA) according to the manufacturer's instructions. In brief, SH-SY5Y cells were seeded in 6-well plates (2×10^5 cells/well), at the end of indicated described, the cells were collected and washed twice with cold PBS. Then 1×10^5 cells were loaded with PI (5 μl final concentration: 50 μg/ml) and Annexin V-FITC (5 μl final concentration: 6 μg/ml) at room temperature for 15 min in the dark and detected by flow cytometer (Becton Dickinson, NJ, USA).

2.8. Intracellular reactive oxygen species (ROS) assay

ROS is one of vital etiological factors of oxidative stress, which could activate the apoptotic cascades. SH-SY5Y cells were cultured in 6-well plates (2×10^5 cells/well) and were collected at the end of indicated treatments. A commercial Reactive Oxygen Species Assay Kit (Beyotime Biotechnology, Nanjing, China) was used to detect the ROS production.

Table 1
The docking score values of the five ligands.

No.	Compound name	LibDock score
Control	Ifenprodil	135
1	Oxypeucedaninhydrabutanolate	140
2	Polygonimitin C	139
3	Kukoamine A	137
4	Loganin	136
5	Harpagide	136

In brief, the cells were incubated with DCFH-DA (10 μM, 37 °C, 20 min), then the cells were washed twice with PBS and intracellular ROS was detected by flow cytometer (Becton Dickinson, NJ, USA) using excitation/emission of 488/525 nm, respectively. All values for each treatment group had been normalized to the control group.

2.9. Superoxide dismutase (SOD) activity and the malondialdehyde (MDA) level

SH-SY5Y cells were cultured in 6-well plates (2×10^5 cells/well) and were collected at the end of indicated treatments. Then the cells were scraped from the plates into ice-cold RIPA analysis buffer (Beyotime Biotechnology, Nanjing, China). Protein concentration was determined by the BCA protein assay kit (Beyotime Biotechnology, Nanjing, China). The determination method of MDA and SOD (Beyotime Biotechnology, Nanjing, China) was conducted according to the manufacturer's protocol.

2.10. Measurement of mitochondrial membrane potential (MMP)

The MMP was a sign of early apoptosis. In our study, MMP was detected by fluorescent dye Rhodamine 123 (Sigma. USA). SH-SY5Y cells were cultured in 6-well plates (2×10^5 cells/well) and were collected at the end of indicated treatments. After that, the cells were dyed with Rhodamine 123 (10 μg/ml) and incubated for 20 min at 37 °C in the dark, after washing twice with PBS, the fluorescence was estimated at an excitation/emission of 485/535 nm by using a flow cytometer (Becton Dickinson, NJ, USA). All values for each treatment group had been normalized to the control group.

2.11. Calcium imaging

Ca^{2+} influx is a momentous mechanism in NMDAR-mediated cell apoptosis. A laser scanning confocal microscope was used to real-time monitor the condition of Ca^{2+} influx. SH-SY5Y cells were cultured in three 3.5 mm plates (2×10^5 cells/well) for 24 h, then KuA (20 μM) was added to the cells, meanwhile, equal DMEM culture fluid was added to the control and model cells for 12 h. After these treatments, the supernatant was discarded and cells were incubated with 2.5 μM fluo-3/AM (Beyotime, China) at 37 °C for 30 min. Then the cells were washed twice using Mg^{2+}-free Extracellular Solution (ECS) containing (in mM): NaCl 140, KCl 3, $CaCl_2$ 2, HEPES 10, glucose 10, adjusted to pH 7.2–7.3 with NaOH and cultured with the original medium for another 30 min. The dye-loaded cells (green fluorescence) were measured with a laser scanning confocal microscope (LEICA). For model group, before being exposed to H_2O_2 (600 μM) or NMDA (1 mM), the dye-loaded cells were scanned for 4 min to obtain a basal level of intracellular Ca^{2+}. Then H_2O_2 or NMDA was applied to the

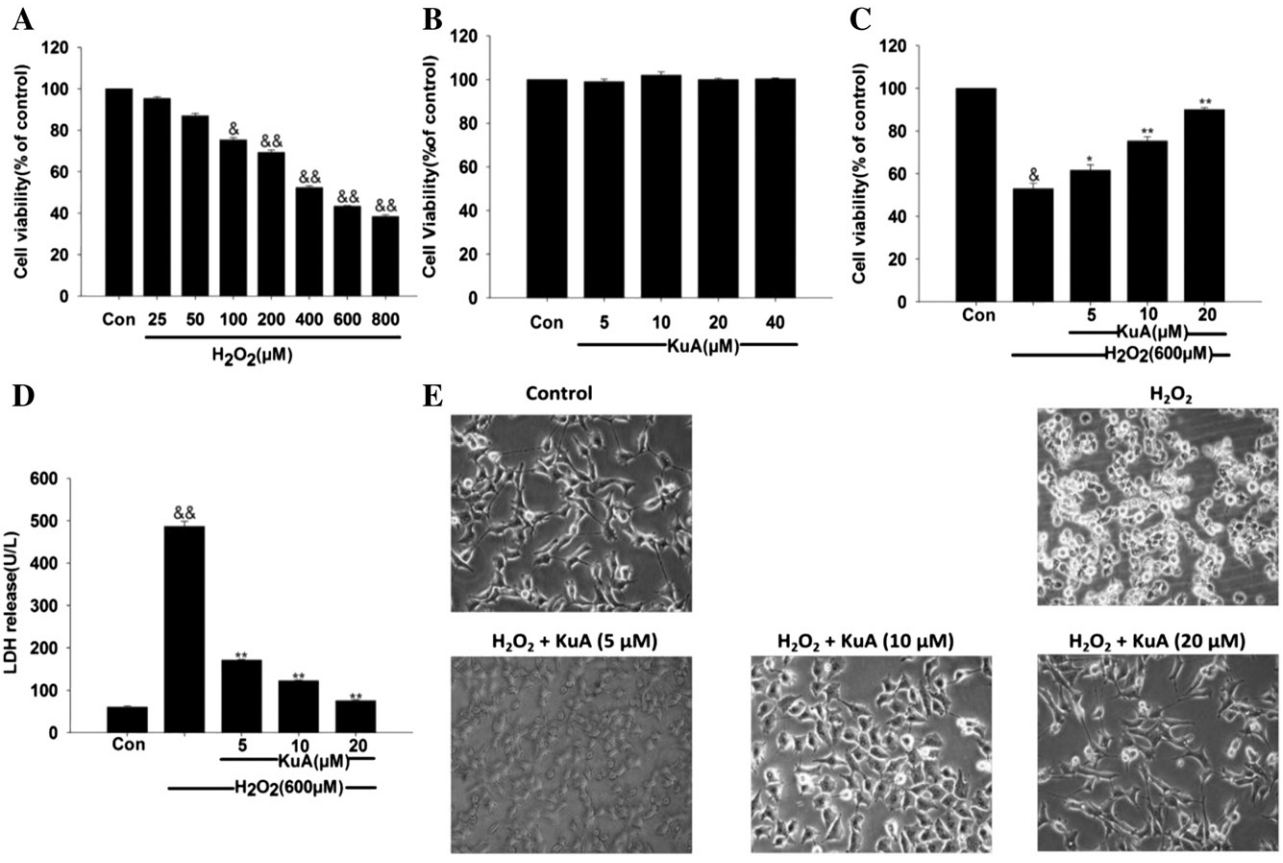

Fig. 2. Neuroprotection of KuA in SH-SY5Y cells. (A) Cytotoxic effect of different concentrations of H_2O_2 in SH-SY5Y cells. (B) 5–40 μM KuA treated alone had no effect on cell viability. (C) Dose-dependent protective effect of pretreatment with KuA against H_2O_2-induced cytotoxicity in SH-SY5Y cells. (D) Protective effect of the plasma membrane damage was analyzed by LDH release. (E) The morphology of the SH-SY5Y cells followed by above treatments with an inverted microscope. All the groups were treated with less than 0.01% DMSO. The data were represented as mean ± S.E.M. of three independent experiments. $^{\&}p < 0.05$ and $^{\&\&}p < 0.01$ compared with control and $^{*}p < 0.05$ and $^{**}p < 0.01$ compared with H_2O_2 treatment cells.

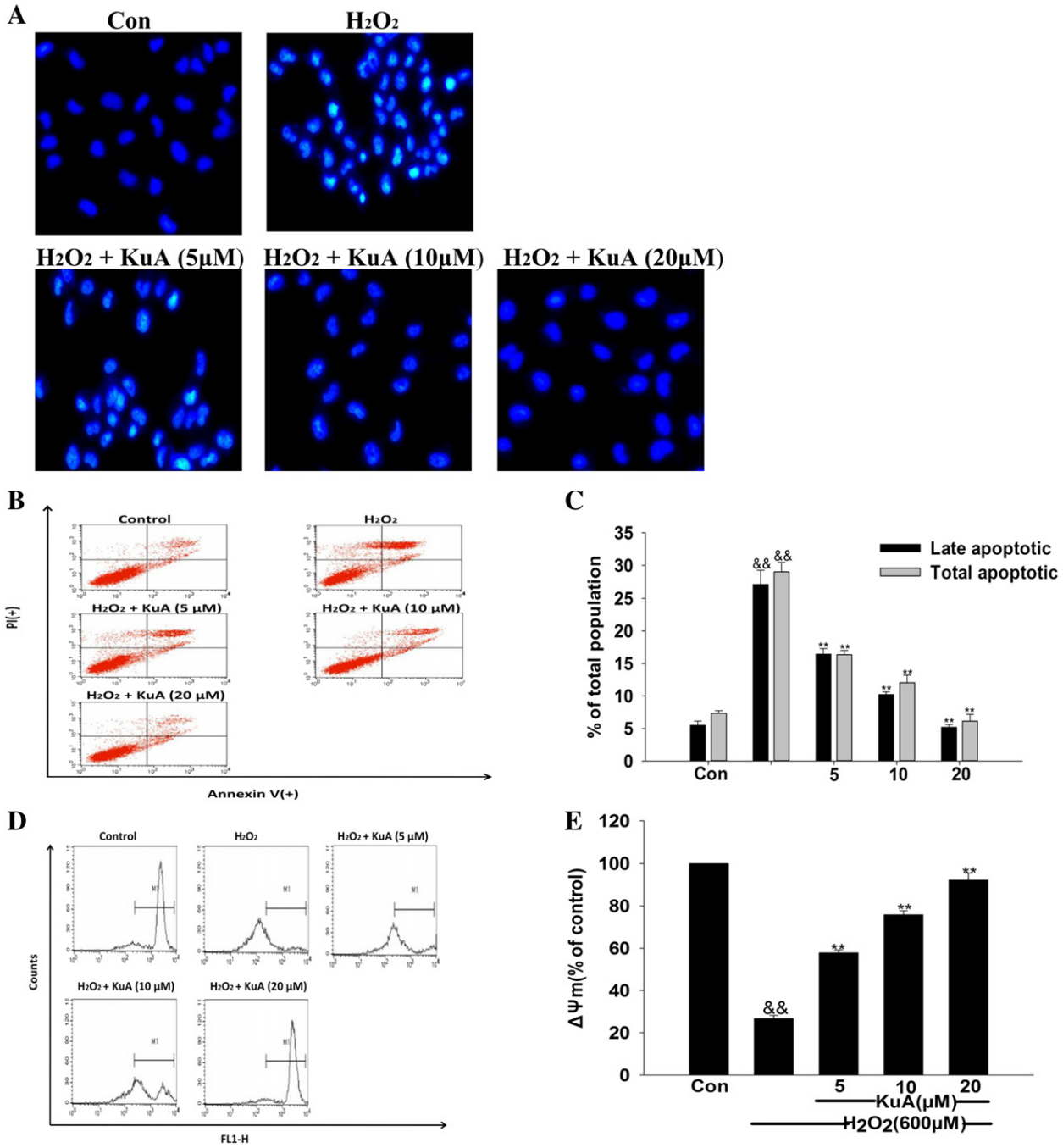

Fig. 3. Effects of KuA on apoptotic and MMP in SH-SY5Y cells. (A) Hoechst 33342 staining (B) Distribution of viable (lower left, Annexin V^- PI^-) necrotic (upper left, Annexin V^- PI^+) late apoptotic (upper right, Annexin V^+ PI^+) and early apoptotic (lower right, Annexin V^+ PI^-) (C) Bar graphs showed the quantitative results of AV-PI. (D) ΔΨm was analyzed by flow cytometry (E) Bar graphs showed the quantitative analysis for MMP. The data were represented as mean ± S.E.M. of three independent experiments. $^{\&}p < 0.05$ and $^{\&\&}p < 0.01$ compared with control and $^{*}p < 0.05$ and $^{**}p < 0.01$ compared with H_2O_2 treatment cells.

cultures. And for the control group, an equal amount of ECS as the H_2O_2 or NMDA in model group was added. The images were recorded every 10s with a laser scanning confocal microscope.

2.12. Western-blot analysis

The potential mechanisms of KuA on NMDARs were verified by western-blot assay. SH-SY5Y cells were cultured in 6-well plates (2×10^5 cells/well) and were collected at the end of indicated treatments. Then the RIPA lysis buffer (1% NP-40, 0.5% deoxycholate, 0.1% SDS) was used to crack the cells for collecting the cytosolic proteins. Protein concentration was determined by BCA assay. The samples containing 50 μg of protein from each treatment condition was separated by SDS/PAGE and transferred to PVDF membranes (Millipore Corporation). Total proteins were blocked with 5% non-fat milk and phosphorylation proteins were blocked with 5% BSA, which were dissolved in TBST for at least 1 h at room temperature. Finally, the membranes were washed three times and incubated with individual primary antibodies (Bax at 1:1000, Bcl-2 at 1:1000, procaspase3 at 1:800, procaspase9 at 1:800, cytochrome c at 1:1000, p53 at 1:800, ERK and p-ERK at 1:800, JNK and p-JNK at 1:800, p38 and p-p38 at 1:800, AKT and p-AKT at 1:800, NR2A and NR2B at

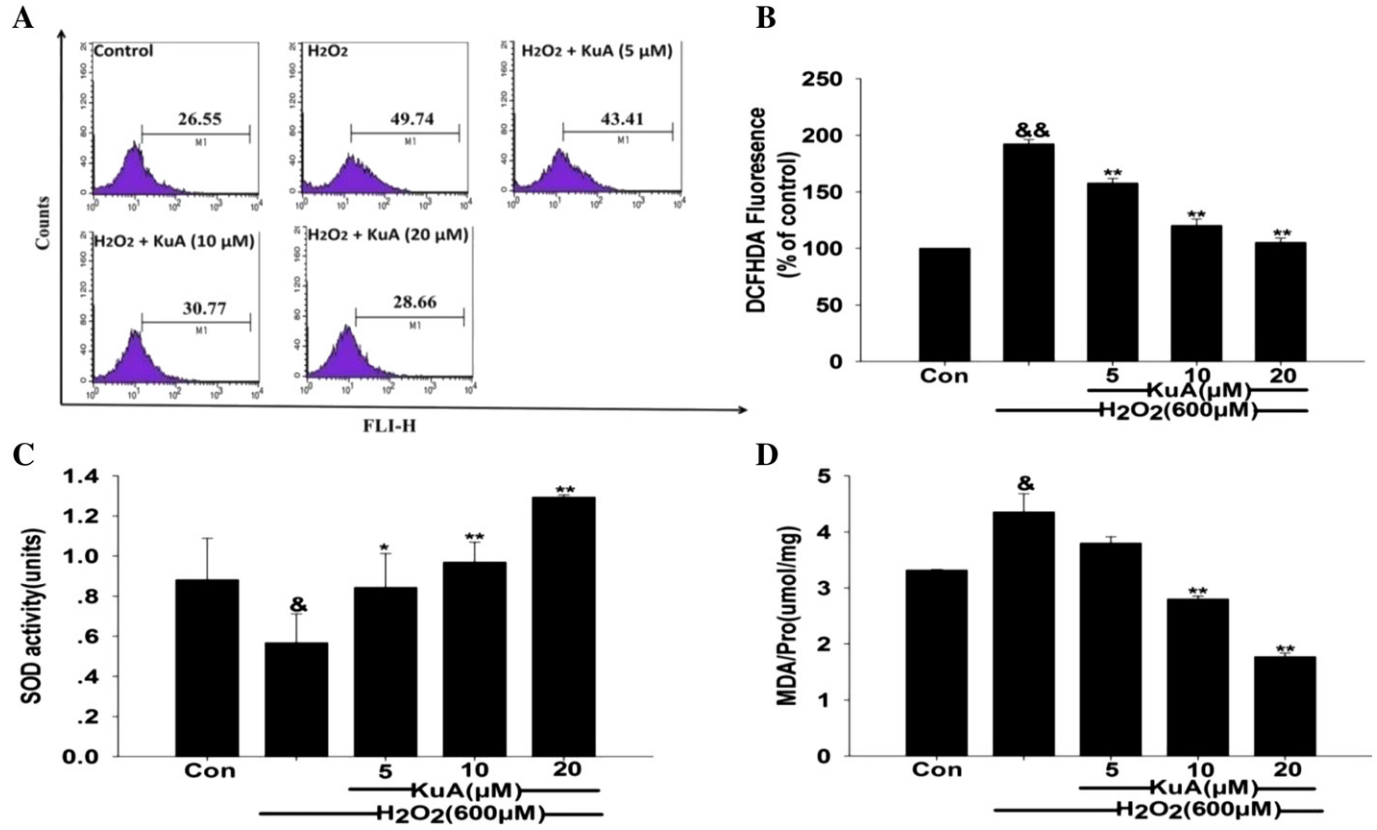

Fig. 4. The effects of KuA on ROS production, SOD activity and MDA level.(A) the intracellular ROS production was detected by flow cytometry. (B) Bar graphs showed intracellular ROS production relative to the control group. (C) Bar graphs represented the activity of SOD. (D) Bar graphs displayed quantitative analysis of MDA level. The data were represented as mean ± S.E.M. of three independent experiments. $^{\&}p < 0.05$ and $^{\&\&}p < 0.01$ compared with control and $^{*}p < 0.05$ and $^{**}p < 0.01$ compared with H_2O_2 treatment cells.

1:1000, CREB and p-CREB at 1:1000) shaking overnight at 4 °C. After three times of washing with TBST buffer, the membranes were incubated with the anti-rabbit or anti-mouse IgG secondary antibody (1:12000) in TBST for 1 h at room temperature, followed by three times of washing. At the end of each treatment the binding of antibody was detected with BeyoECL Plus. The results were expressed as the percentage of control, which was deemed to be 100%.

2.13. Statistical analysis

Data were analyzed by SigmaPlot 12.5 software and the results were represented as the mean ± S.E.M. Statistical significance was analyzed with one-way analysis of variance followed by a Tukey's HSD-post hoc test. Differences with p value less than 0.05 were considered statistically significant.

3. Results

3.1. Virtual screen of the TCM database to find potential NMDAR antagonists

Molecular docking was used to get potential NMDAR antagonists from virtual screening of TCM database [14]. The Lipinski rule (Mr ≤ 500, log P ≤ 5, hydrogen bond donor groups ≤ 5, hydrogen bond acceptor groups ≤ 10) [17] and the LibDock score, which are a comprehensive scoring function in DS 3.0 software were used to screen the appropriate compounds. Its ligand, ifenprodil, was conducted as a control. According to the rule and LibDock score, we chose the most suitable five compounds (Table 1), and these compounds were proceeding to detect the cell survival of H_2O_2-induced cell apoptosis by MTT assay. As a result, KuA exerted the best neuroprotection among the five compounds. (Data are not shown).

3.2. KuA prevents SH-SY5Y cells from H_2O_2-induced cytotoxicity

Just like in Section 3.1, KuA exhibited the best neuroprotective activity. As shown in Fig. 2A, H_2O_2 decreased cell viability in a dose-dependent manner. Different concentrations of KuA alone cannot affect the cell viability (Fig. 2B). The effect of KuA against H_2O_2-induced cell death was shown in Fig. 2C, after being exposed to 600 μM of H_2O_2 for 3 h, cell viability was reduced to 53.00 ± 2.60% of control. Pretreatment with KuA (5, 10, 20 μM) could prevent cell death and improve cell viability to 61.66 ± 2.51%, 75.33 ± 2.08%, and 90.01 ± 1.00% of control, respectively. The neurotoxicity of H_2O_2 and the protective effect of KuA were further evaluated by LDH assay. As shown in Fig. 2D, the LDH release in H_2O_2-stimulated group (480.66 ± 12.02 U/L) was much more than the control group (60.33 ± 2.60 U/L). In contrast, KuA (5, 10, 20 μM) pretreatment lowered the LDH release in a dose-dependent manner (171.00 ± 1.53, 122.00 ± 1.86, 75.66 ± 1.86 U/L). The protective effect of KuA was further confirmed morphologically by an inverted microscope (Fig. 2E), control cells exhibited uniformly dispersed chromatin, normal organelle and intact cell membrane. Cell exposure to 600 μM of H_2O_2 for 3 h showed typical characteristics of apoptosis, including the condensation of chromatin, the shrinkage of nuclear and the appearance of apoptotic bodies. However, the number of cells with nuclear condensation and fragmentation were markedly decreased when the cells pretreated KuA (5, 10, 20 μM) for 12 h. Hoechst 33342 staining shows that many small bright blue dots representing DNA condensation or nuclear fragmentation were observed after cells were treated with H_2O_2 for 3 h. However,

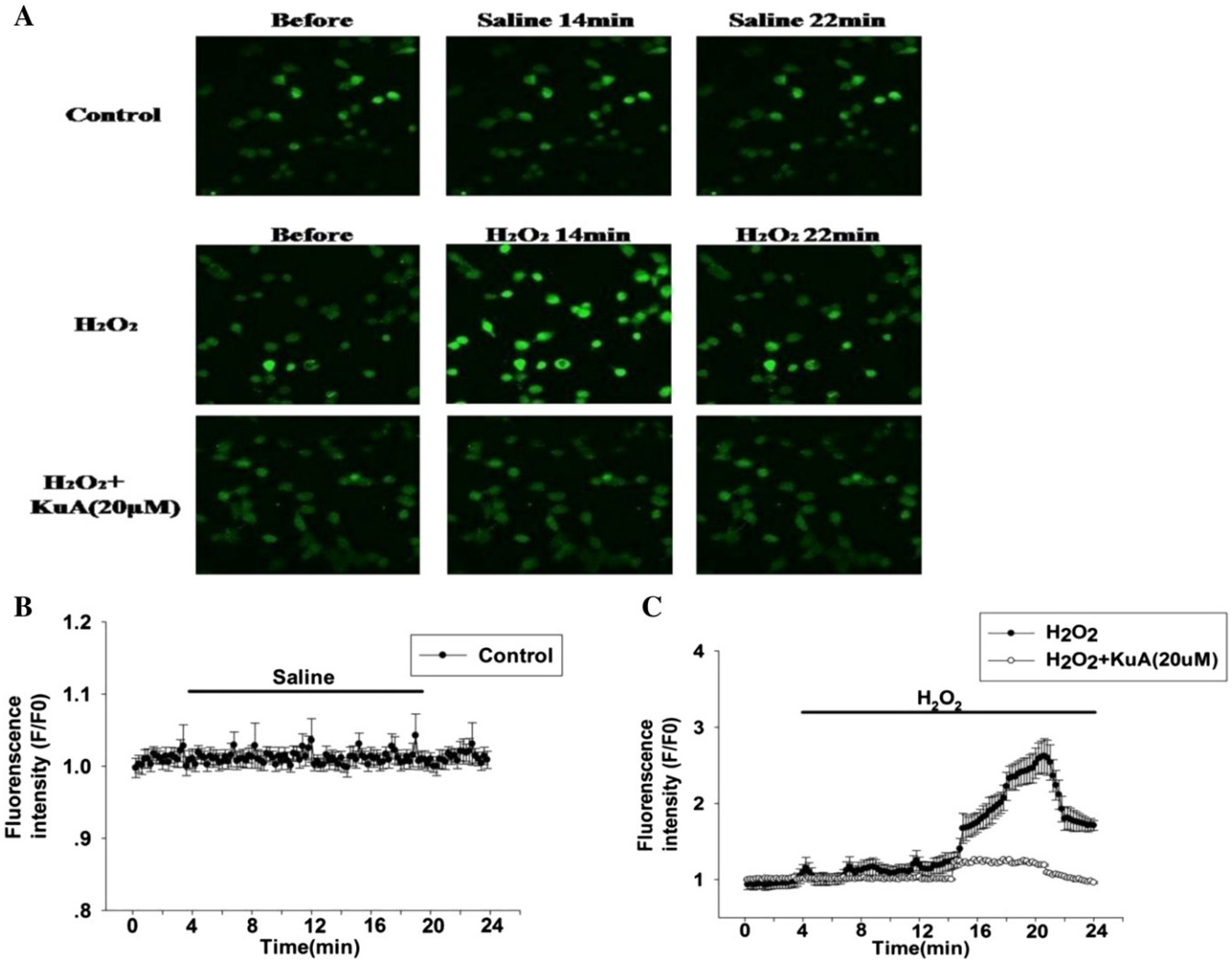

Fig. 5. H_2O_2-induced calcium imaging of SH-SY5Y cells. (A) The green fluorescence under the laser scanning microscope at different times showed the concentration of calcium in SH-SY5Y cells, which was stable during the experiment. (B) The control group fluorescence intensity of the Ca^{2+} was stable during detection by a laser scanning microscope (n = 15 cells). (C) 600 μM of H_2O_2 was able to evoke strong fluorescence intensity (n = 15 cells) and 20 μM of KuA (n = 15 cells) significantly reduced the fluorescence intensity in SH-SY5Y cells.

pretreatment with KuA attenuated these features of apoptosis, indicating that KuA has an anti-apoptotic effect in H_2O_2-treated cells (Fig. 3A).

3.3. KuA attenuated H_2O_2-induced apoptosis and ΔΨm loss in SH-SY5Y cells

Hoechst33342 staining was performed to investigate whether KuB inhibited H_2O_2-induced cell apoptosis. As shown in Fig. 3A, DNA condensation and nuclear fragmentation were presented in cells treated with H_2O_2. However, pretreatment with KuB inhibited these characteristics of apoptosis.

AnnexinV-PI double staining assay was used to further distinguish the features of apoptotic and necrotic cells in response to H_2O_2 with or without KuA. As shown in Fig. 3B and C, a typical representative dot plot analysis of control cells showed total apoptotic cells (7.34 ± 0.39% $p < 0.01$) and late apoptotic cells (5.50 ± 0.64% $p < 0.01$). Compared with the control, H_2O_2 significantly increased the number of total apoptotic cells (29.00 ± 1.47% $p < 0.01$) and late apoptotic cells (27.14 ± 2.1% $p < 0.01$). Pretreatment with KuA (5, 10, 20 μM) decreased total apoptotic cells (17.00 ± 0.66% $p < 0.01$) and late apoptotic cells (16.43 ± 0.86% $p < 0.01$); total apoptotic cells (12.04 ± 1.17% $p < 0.01$) and late apoptotic cells (10.21 ± 0.41% $p < 0.01$); and total apoptotic cells (6.13 ± 1.03% $p < 0.01$) and late apoptotic cells (5.18 ± 0.43% $p < 0.01$), respectively. These data showed that KuA protects SH-SY5Y cells by attenuating H_2O_2-induced apoptosis.

The effect of KuA on H_2O_2-induced ΔΨm loss was examined by flow cytometry. As shown in Fig. 3D, KuA could increase the MMP. KuA could improve the MMP to 49.88 ± 1.11%, 76.43 ± 0.79%, and 91.56 ± 1.35%, respectively against H_2O_2-induced ΔΨm (31.33 ± 2.12%) loss in a dose-dependent manner (Fig. 3E). The data were expressed as the ratio comparing to control. All the results indicated that KuA attenuated the cell apoptosis by enhancing the ΔΨm.

3.4. KuA attenuated the ROS production and the MDA level and improved the SOD activity in SH-SY5Y cells

To determine the effect of KuA on the ROS generation induced by H_2O_2, we performed flow cytometry analysis using the ROS-sensitive fluorescence probe, DCFH-DA. The results were shown in Fig. 4A and B, exposure to H_2O_2 could cause an elevation of the intracellular ROS, which was about 2.0-fold relative to that of control cells. Pretreatment with KuA (5, 10, 20 μM) suppressed the elevation of intracellular ROS. These results indicated that KuA had the ability to scavenge ROS induced by H_2O_2.

To examine the SOD activity, the principle of the method was based on the inhibition of NBT reduction by the xanthine–xanthine oxidase system as a superoxide generator. As shown in Fig. 4C, being exposed

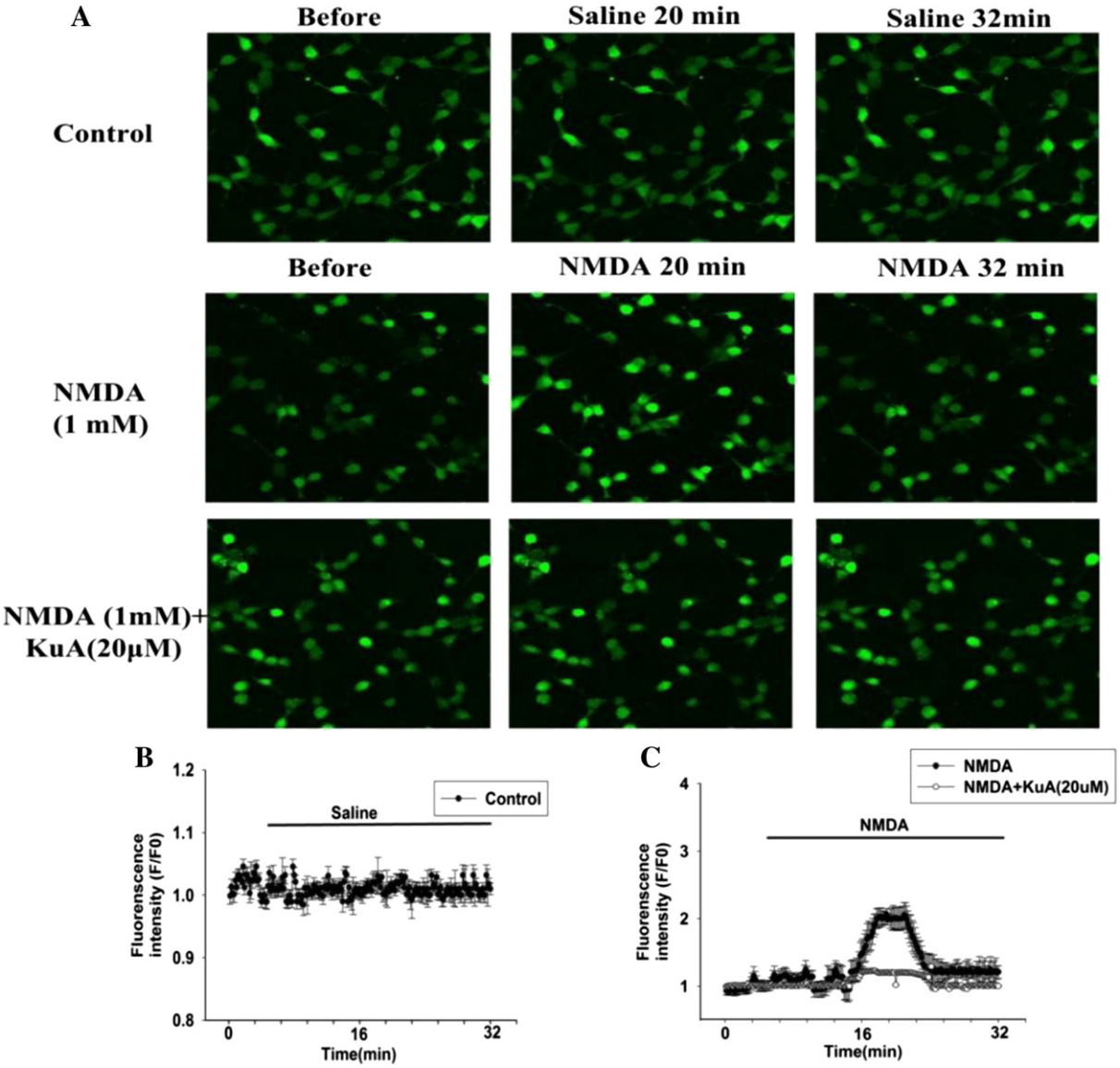

Fig. 6. NMDA-induced calcium imaging of SH-SY5Y cells. (A) The green fluorescence under the laser scanning microscope at different times showed the concentration of calcium in SH-SY5Y cells, which was stable during the experiment. (B) The control group fluorescence intensity of the Ca^{2+} was stable during detection by a laser scanning microscope (n = 15 cells). (C) NMDA (1 mM) was able to evoke strong fluorescence intensity (n = 15 cells) and 20 μM of KuA (n = 15 cells) significantly reduced the fluorescence intensity in SH-SY5Y cells.

to H_2O_2 could cause a reduction of the SOD activity to 0.56 ± 0.15 units compared with control cells, and pretreatment with KuA (5, 10, 20 μM) could improve the SOD activity effectively. The results indicated that KuA could prevent the decrease of H_2O_2-induced SOD activity.

The MDA level was tested according to the red production of MDA and TBD reaction, measured by Microplate Reader. The result was shown in Fig. 4D that H_2O_2-stimulated could increase the MDA level to 4.4 ± 0.33 μmol/mg, and pretreatment with KuA (5, 10, 20 μM) for 12 h could decrease the MDA level significantly. The results suggested that KuA could prevent the increase of H_2O_2-induced MDA level.

3.5. KuA decreased H_2O_2-induced Ca^{2+} influx in SH-SY5Y cells

A laser scanning microscope was used to detect the Ca^{2+} in SH-SY5Y cells after H_2O_2 exposure, the calcium concentration in SH-SY5Y cells with or without H_2O_2 and KuA was detected (Fig. 5A, B and C). The fluorescence intensity can be regarded as an indicator of cytoplasmic Ca^{2+} concentration. The concentration of Ca^{2+} in SH-SY5Y was stable during our detection time, and H_2O_2 (600 μM) evoked an elevation of Ca^{2+} concentration in SH-SY5Y cells. However, the slow reduction in the next 22 min stayed at a relatively higher stage. Pretreatment with KuA (20 μM) could attenuate calcium influx after H_2O_2 exposure.

3.6. KuA decreased NMDA-induced Ca^{2+} influx in SH-SY5Y cells

NMDA-induced Ca^{2+} influx in SH-SY5Y cell model was used to state the links between KuA and NMDARs. As shown in Fig. 6A, the intracellular Ca^{2+} was kept at a stable level. However, NMDA (1 mM) evoked an elevation of Ca^{2+} concentration in SH-SY5Y cells. It kept a high stage from 18 min to 26 min (Fig. 6B). And pretreatment with KuA (20 μM) could attenuate calcium influx after NMDA exposure (Fig. 6C).

3.7. KuA modulated H_2O_2-induced apoptosis-related protein expression in SH-SY5Y cells

The expression of apoptosis-related proteins, including Bcl-2, Bax, cytochrome c, procaspase-3, procaspase-9 and p53 were detected by western-blot assay and β-actin was served as the internal standard. As shown in Fig. 7A, compared with the H_2O_2 alone group, pretreatment

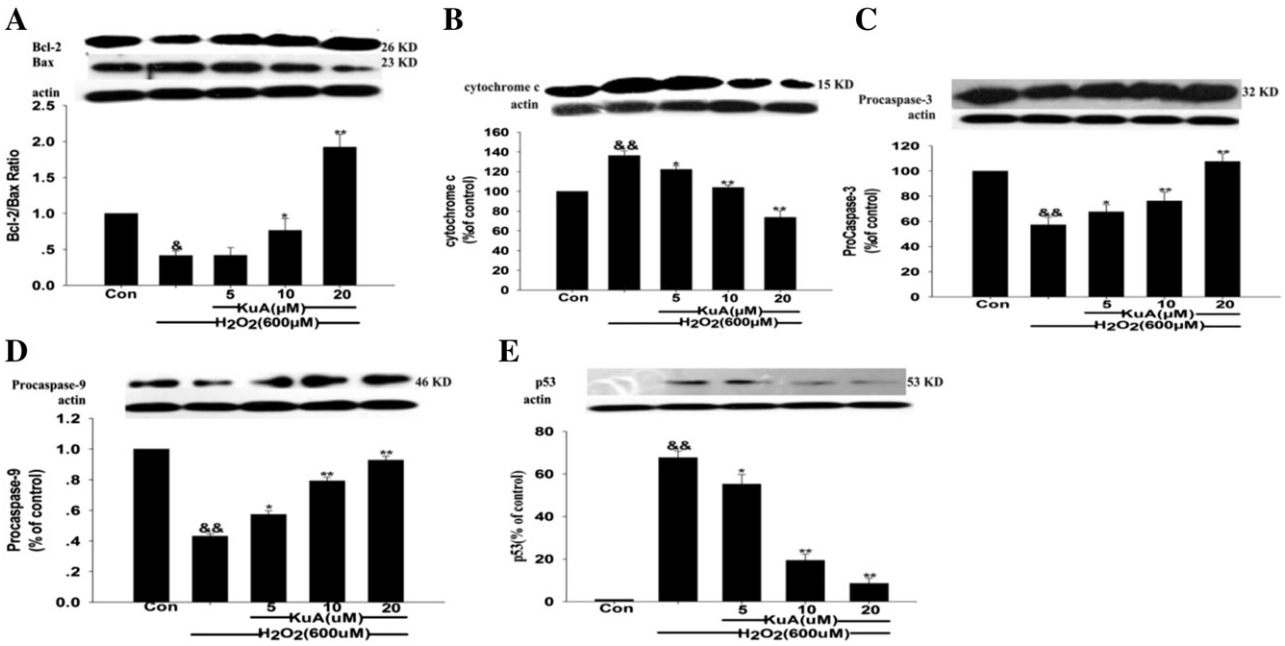

Fig. 7. KuA regulated the expression of H_2O_2-induced apoptosis-related proteins in SH-SY5Y cells. Western blot and quantitative analyses for (A) the expression of Bcl-2 and Bax and their ratio; (B) the expression of cytochrome c; (C) the expression of procaspase-3; (D) the expression of procaspase-9; and (E) the expression of p53. The data were represented as mean ± S.E.M. of three independent experiments. $^{\&}p < 0.05$ and $^{\&\&}p < 0.01$ compared with control and $^{*}p < 0.05$ and $^{**}p < 0.01$ compared with H_2O_2 treatment cells.

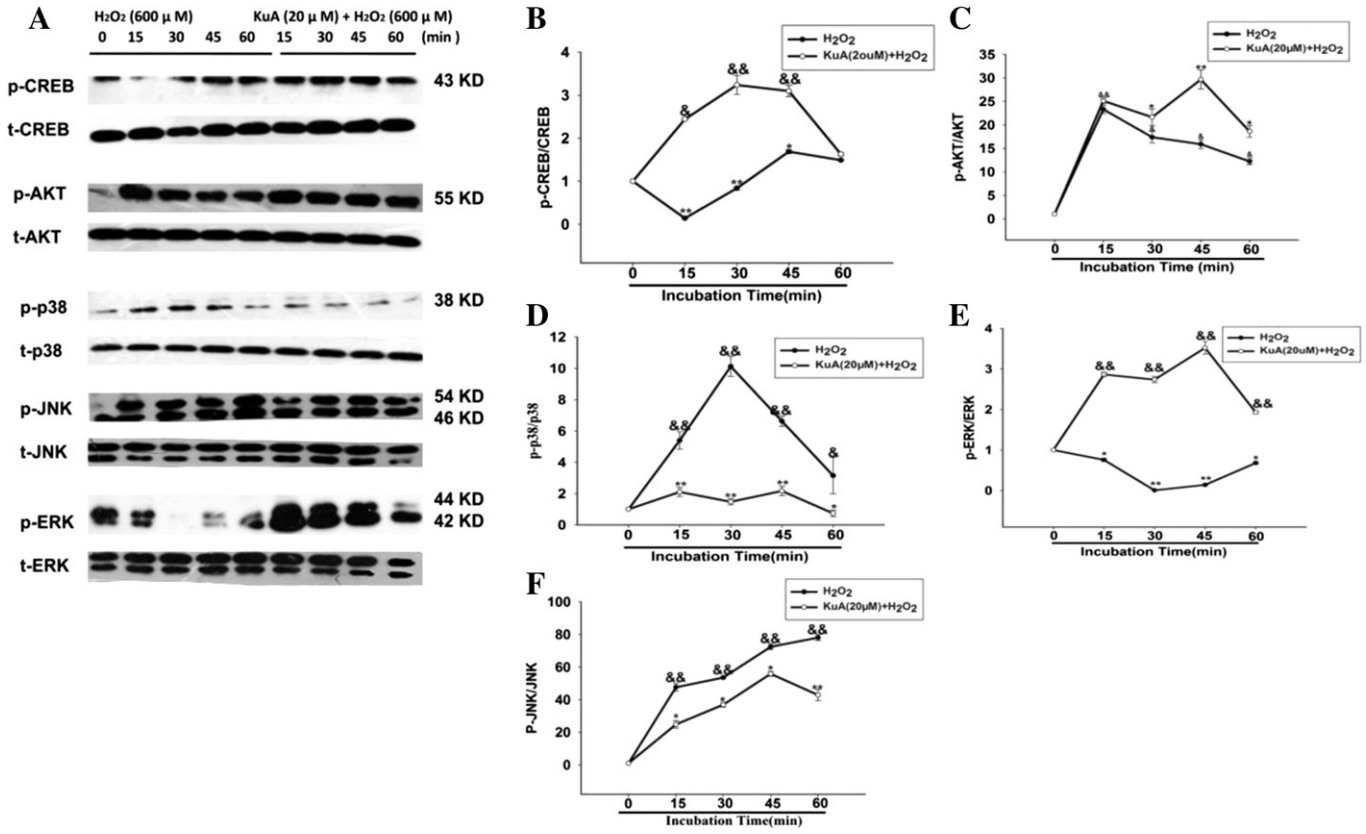

Fig. 8. KuA on the expression of MAPKs, AKT and CREB in SH-SY5Y cells. The cells were incubated with KuA (20 μM) for 12 h, then stimulated with or without H_2O_2 (600 μM) for indicating periods. (A) The bands of phosphor- and total-ERK1/2, JNK1/2, p38, AKT and CREB. (B) Curve charts showed a quantitative analysis of p-AKT/AKT, p-p38/p38, p-JNK1/2/JNK1/2, p-ERK1/2/ERK1/2 and p-CREB/CREB, respectively. The data were represented as mean ± S.E.M. of three independent experiments. $^{\&}p < 0.05$ and $^{\&\&}p < 0.01$ compared with control and $^{*}p < 0.05$, $^{**}p < 0.01$ compared with H_2O_2 treatment cells.

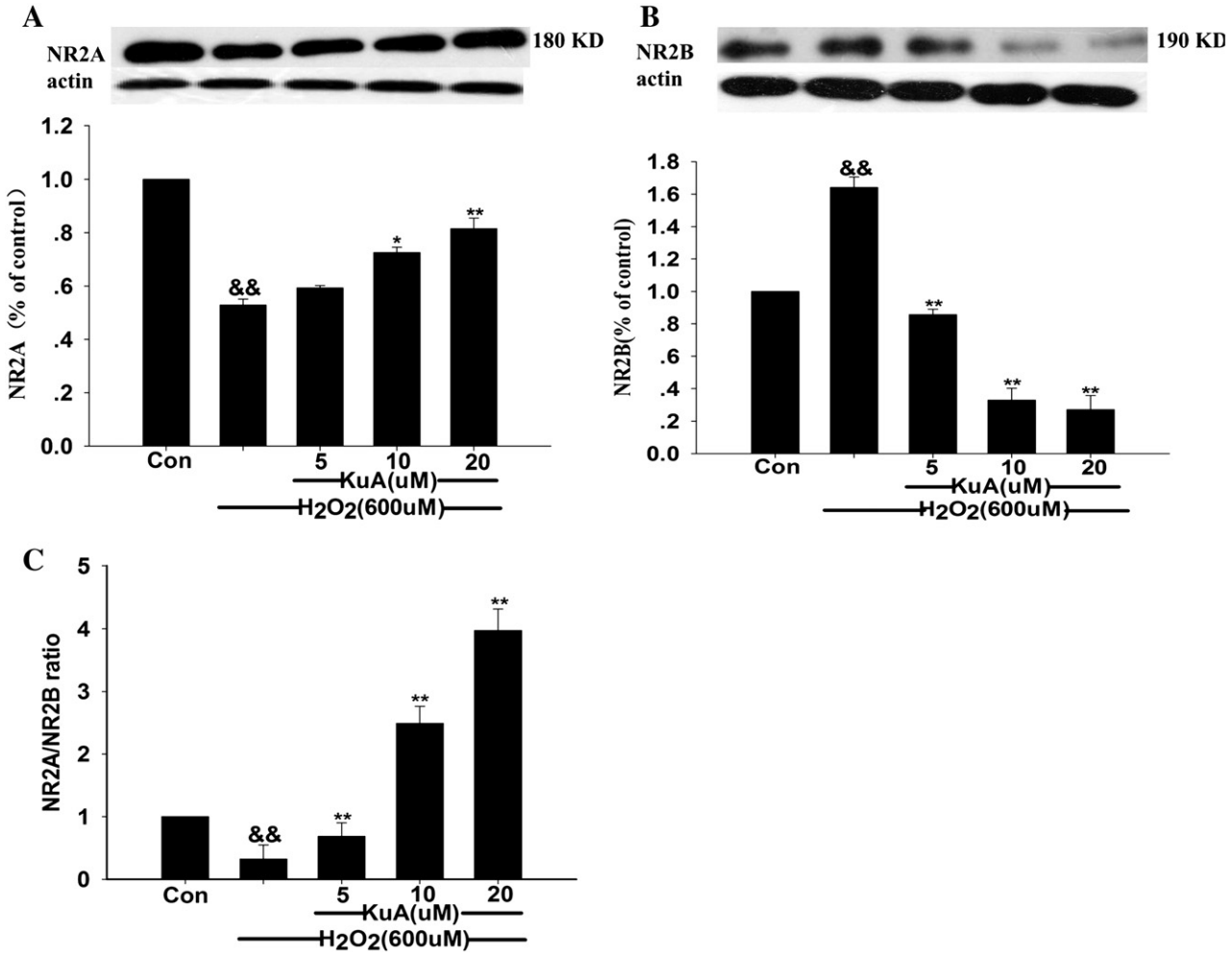

Fig. 9. Effects of KuA on the expression of NR2A and NR2B, which were detected by western-blot assay, and the quantitative analysis for (A) the expression of NR2A, (B) the expression of NR2B, and (C) the NR2A/NR2B ratio. The data were represented as mean ± S.E.M. of three independent experiments. $^{\&}p < 0.05$ and $^{\&\&}p < 0.01$ compared with control and $^{*}p < 0.05$, $^{**}p < 0.01$ compared with H_2O_2 treatment cells.

with KuA significantly increased the ratio of Bcl-2/Bax. KuA can also increase the expression of procaspase-3 and procaspase-9 in a dose-dependent manner (Fig. 7B). In contrast, the high levels of cytochrome c and p53 observed in the H_2O_2 group were decreased with KuA pretreated in a dose-dependent manner (Fig. 7C–E).

3.8. The effects of KuA on the expression of MAPKs, AKT and CREB in SH-SY5Y cells

To identify the mechanisms of anti-apoptosis by KuA, the expression of MAPKs, AKT and CREB were measured by western-blot assay. There were almost no detectable phosphorylation of p38, JNK1/2, and AKT in unstimulated cells, while pretreatment with KuA (5, 10, 20 μM) could decrease the phosphorylation of p38 and increase the phosphorylation of ERK1/2, AKT and CREB. However, KuA had little influence on the expression of JNK1/2 (Fig. 8A–F) These results suggested that KuA decreases cell apoptosis involved in ERK1/2, p38, AKT and CREB pathways.

3.9. Effects of KuA on the expression of NR2A- and NR2B-containing NMDARs

As it represented in Fig. 9A and B, the results of western-blot showed that exposure to H_2O_2 could decrease the expression of NR2A subtype and increase the expression of NR2B subtype in SH-SY5Y cells, whereas pretreatment with KuA (5, 10, 20 μM) for 12 h significantly increased the expression of NR2A subtype and decrease the over expression of NR2B subtype induced by H_2O_2 in a dose-dependent manner. KuA could also increase the ratio of NR2A/NR2B (Fig. 9C).

3.10. Molecular docking simulated the interaction between KuA and NMDARs

To gain further insight into the interaction mechanisms between KuA and NMDARs, computational docking was performed to dock KuA with NMDARs. In the KuA-NMDAR complex, hydrogen bonds were formed at the KuA moiety with the active residues Gln110, Ala107 and Asn334 in the pocket. And the Tyr109 can also form π–π stacking interaction with KuA. (Fig. 10A, B and C).

4. Discussion

The present study identified that treatment with KuA could reduce apoptotic cell death in H_2O_2-stimulated SH-SY5Y cells. Our data showed that the potential mechanisms of this anti-apoptotic performance were partly involved in NMDARs. In addition, NMDA-stimulated SH-SY5Y cell model suggested that KuA restrained Ca^{2+} influx. Then how does KuA achieve an antioxidant effect and how is the relationship of KuA and NMDARs?

As is known to all, Oxygen free radicals and lipid peroxidation are believed to play vital roles in neuronal cell death [18,19]. Actually, a lot of studies suggest that excitatory amino acids (EAAs) and lipid

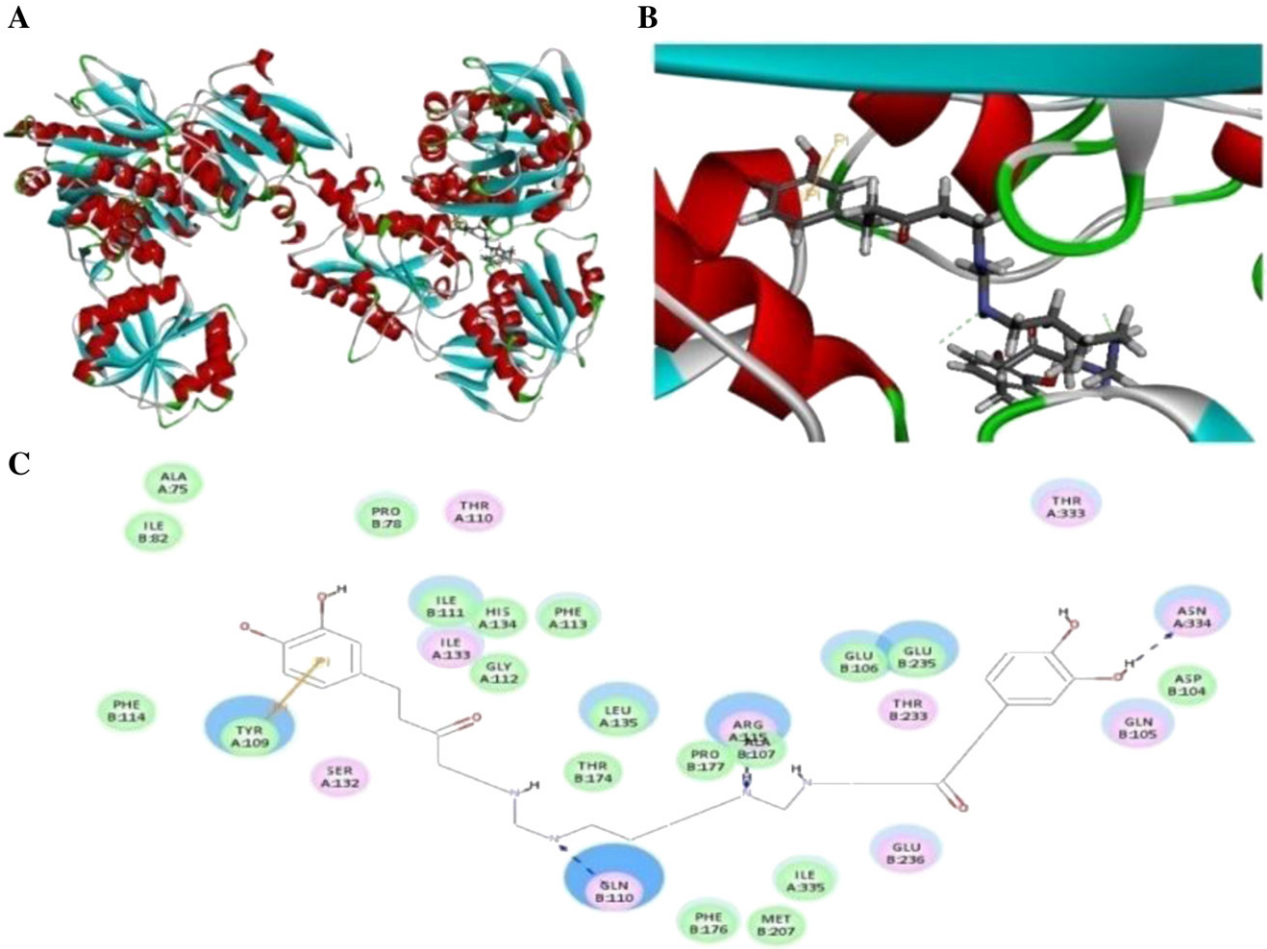

Fig. 10. Molecular docking for the interaction between KuA and NR2B-containing NMDARs. Representative binding mode of the most stable docking poses of KuA with NMDARs. (A) The complete view of the docking pose of KuA. NMDARs were expressed as a solid ribbon diagram and KuA as a stick depiction. (B) The close-up view of the calculated KuA-NMDAR complex docking modes. (C) The two-dimensional diagram of KuA combines with NMDARs. Hydrogen bond interactions between KuA and NMDAR residues were presented as blue dots and π–π stacking interaction between them were presented as red full line.

peroxidation interact with each other and lead to cell death as a ripple effect showed that MDA increases significantly in the injured hemisphere. SOD represents the most important line of defense against oxidative stress catalyzing the dismutation reaction of superoxide anion to hydrogen peroxide. In our study, treatment with KuA increased the reduced activity of SOD and decreased the MDA level. This indicated that KuA effectively confront the oxidative stress in the first place.

Mitochondrial dysfunction is the sign of early apoptosis in both H_2O_2 and NMDAR-induced cell apoptosis. As described previously, mitochondrial membrane permeabilization, which directly affects the mitochondrial membrane potential (MMP), regulated by proteins of Bcl-2 family is considered as irreversible apoptotic pathway [20,21]. The anti-apoptotic factor Bcl-2, residing in the outer mitochondrial membrane, inhibits cytochrome c release and the pro-apoptotic factor Bax residing in the cytosol and promotes the mitochondrial membrane permeabilization, delivering apoptotic signaling when translocates from the cytoplasm to the mitochondria [22]. Increasing mitochondrial permeabilization results in the release of cytochrome c from the mitochondria [23] and releasing cytochrome c triggers activation of caspase-9 and then the caspase-9 activates caspase-3, which induces cell death. Meanwhile, mitochondrial dysfunction leads to mitochondrial ROS easily spreading throughout the cytoplasm, further resulting in intracellular ROS generation, and creating a free radical vicious cycle of injury [24]. Our data showed that KuB prevented H_2O_2-induced intracellular ROS production, $\Delta\Psi_m$ loss, caspase-9 and caspase-3 degradation. In addition, decreasing Bcl-2/Bax ratio could be used to indicate the state of mitochondria [25,26]. Oxidative stress causes neuronal apoptosis which was strengthened by the pro-apoptotic factor p53, which could further lower the Bcl-2/Bax ratio [27]. In the same way, the high expression of p53 in H_2O_2-stimulated cells was also reduced by KuB. Altogether, the present data indicated that KuB provides neuroprotection via the preservation of mitochondrial function in SH-SY5Y cells.

Activated intracellular JNK and p38 signaling were involved in regulating many cellular events such as oxidative-stress induced cell death [26,28]. Thus we studied the effect of KuA on H_2O_2-induced phosphorylative p38 and JNK1/2. Consisting with the previous study that H_2O_2 has the capacity of activating p-p38, p-JNK1/2 and studies have shown that JNK is also related to neuronal cell death [29], but our data showed that KuA could only inhibit the phosphorylation of p38 while had little effect on the expression of p-JNK1/2. These results indicated that the protective effect of KuA on H_2O_2-induced cell injury was regulated via p38 SAPK dependent pathway. In contrast to p38, AKT, a pathway downstream of PI3K, is a key factor to regulate cell survival after cerebral ischemia and could phosphorylate procaspase-9 which could ulteriorly inhibit the caspase family [30,31]. This is consist with our results that KuA could increase the expression of p-AKT and further influence caspase expression compare with H_2O_2-stimulated group. At the same time, the ERK-CREB pathway, which regulates transcription of potential neuroprotective genes, such as Bcl-2 and brain derived neurotrophic factor is most frequently associated with cell survival activity [32,33]. Our data showed that H_2O_2 could inhibit

the phosphorylation of AKT, CREB and ERK1/2, however, pretreatment with KuA could reverse this tendency. It preliminarily indicated that KuA provided neuroprotection which might involve in PI3K/AKT and ERK/CREB signaling pathway. In addition, previous study have shown that activated NR2B-containing NMDARs could inactivate ERK/CREB [34] and our result revealed that H_2O_2-stimulated SH-SY5Y cells increased the NR2B expression but pretreatment with KuA could downregulate NR2B and upregulate p-ERK and p-CREB expression. This is to largely extent indicated the anti-apoptotic induced by H_2O_2 might via NMDARs and further influenced the ERK/CREB pathway.

All the results suggested that KuA has anti-oxidative stress ability. However, as mentioned previously that NMDARs were used as a target in our screening, so whether KuA has effect on this receptor and whether its anti-oxidative stress via NMDARs is very exciting. A lot of research has detected the expression of NMDA receptors in SH-SY5Y cell lines and the cell was being used to study NMDARs by some individuals [35–38]. It has been reported that H_2O_2 could activate NMDARs which could further lead to intracellular calcium overload [39,40]. Therefore, we treated SH-SY5Y cells with H_2O_2 again in our subsequent experiments and the expression of NR2A, NR2B and the concentration of intracellular Ca^{2+}, which is the first step of NMDAR activation, was detected to assess the effect of KuA on NMDARs. To our joy that the data showed KuA could effectively prevent Ca^{2+} influx compare with H_2O_2 group and we ulteriorly found that KuA could also upregulate NR2A expression, downregulate NR2B expression and increase the ratio of NR2A/NR2B (Fig. 9C). These results suggested that KuA prevent H_2O_2-induced cell death might involved in NMDAR-Ca^{2+} pathway. However, H_2O_2 not a specific NMDAR agonist and it might via generating oxidative stress, which promotes the tyrosine phosphorylation of NMDAR subunits and increased tyrosine phosphorylation of NMDAR subunits has been reported to potentiate receptor function and exacerbate NMDAR-induced cell injury [41]. Therefore, N-methyl-D-aspartate (NMDA), a NMDAR agonist, was used to further verify the blockade effect of KuA on NMDARs. Ditto, the result of calcium image indicated that KuA could restrain NMDA-induced calcium influx effectively. Both H_2O_2 and NMDA-induced model explained that KuA might have a potential capacity of blocking NMDARs. But what is the possible combination mode and how is the combined? LibDock/DS was utilized to simulate the relationship of KuA-NMDAR complex. Promisingly, the result showed that there are three hydrogen bonds and one π–π stacking that were formed at the KuA moiety. It suggested that KuA could well combine with NR2B-containing NMDARs and at least 17 active residues existed in the catalytic unit of NMDARs, including Tyr109, Ser132, Gln110, Ile335, Glu236, Gln105, Asp104, Asn334, Glu106, Glu235, Thr233, Ala107, Arg115, Pro177, Thr174, Gly112 and Ile133. These active residues make KuA stably locate in the active pocket of NMDARs. Further, as shown in Fig. 10C, the four active residues directly connected with KuA, Gln110, Ala107, Asn334 and Tyr109, existing in the active pocket were might be potential new key residues for NMDARs.

5. Conclusions

In summary, we believed that the neuroprotective effect of KuA was demonstrated for the first time. The anti-oxidative stress ability of KuA was verified by H_2O_2-induced cell injury model and the potential mechanisms of its anti-oxidative stress may involve in mitochondrial-apoptosis pathway, p38 SAPK pathway and NR2A, NR2B-containing NMDA receptor. The result of NMDA-induced Ca^{2+} influx and molecular docking showed that KuA simultaneously has the ability of blocking NMDARs. Therefore, we boldly speculate that the anti-oxidative stress of KuA may not only be an antioxidant to itself but also via NMDARs and these make KuA to be a candidate for ischemic stroke therapy. However, the existing experiment results cannot adequately demonstrate KuA as a NMDARs antagonist, so in vitro and in vivo research will be further studied.

6. Conflict of interest

There no conflicts of interest to declare.

Acknowledgements

This work was supported by the National Science and Technology Major Project, People's republic of China (Project number: 2014ZX09J14101-05C).

References

[1] M. Daher, Overview of the world health report 2000 health systems: improving performance, J. Med. Liban. 49 (2001) 22–24.
[2] S.L. Mehta, N. Manhas, R. Raghubir, Molecular targets in cerebral ischemia for developing novel therapeutics, Brain Res. Rev. 54 (2007) 34–66.
[3] A.S. Hazell, Excitotoxic mechanisms in stroke: an update of concepts and treatment strategies, Neurochem. Int. 50 (2007) 941–953.
[4] J.M. McCord, Oxygen-derived free radicals in post-ischemic tissue injury, N. Engl. J. Med. 312 (1985) 159–163.
[5] H. Xu, N. Shao, M. Zhang, Experimental study on multi-infarct dementia treated with reinforcing essence to refresh mental activity method, Zhongguo Zhong Xi Yi Jie He Za Zhi 19 (1999) 359–362.
[6] A.M. Brennan, S.W. Suh, S.J. Won, NADPH oxidase is the primary source of superoxide induced by NMDA receptor activation, Nat. Neurosci. 12 (2009) 857–863.
[7] G.E. Hardingham, H. Bading, The Yin and Yang of NMDA receptor signaling, Trends Neurosci. 26 (2003) 81–89.
[8] N.C. Danbolt, J. Storm-Mathisen, B.I. Kanner, An [Na^+ + K^+]coupled L-glutamate transporter purified from rat brain is located in glial cell processes, Neuroscience 51 (1992) 295–310.
[9] E. Shohami, E. Beit-Yannai, M. Horouitz, Oxidative stress in closed-head injury: brain antioxidant capacity as an indicator of functional outcome, J. Cereb. Blood Flow Metab. 17 (1997) 1007–1019.
[10] J.M. Weinberger, Evolving therapeutic approaches to treating acute ischemic stroke, J. Neurol. Sci. 249 (2006) 101–109.
[11] G. Deuschl, P. Krack, C. Schade-Brittinger, A randomized trial of deep-brain stimulation for Parkinson's disease, N. Engl. J. Med. 355 (2006) 1289.
[12] Pripp Are Hugo, Docking and virtual screening of ACE inhibitory dipeptides, Eur. Food Res. Technol. 225 (2007) 589–592.
[13] Sugunadevi Sakkiah, Sundarapandian Thangapandian, Pharmacophore based virtual screening, molecular docking studies to design potent heat shock protein 90 inhibitors, Eur. J. Med. Chem. 46 (2011) 2937–2947.
[14] C.Y. Chen, TCM Database@TaiWan: the world's largest traditional Chinese medicine database for drug screening in silico, PLoS One 6 (2011) 1–5.
[15] S. Funayama, K. Yoshida, C. Konno, Structure of kukoamine A, a hypotensive principle of *Lycium chinense* root barks, Tetrahedron Lett. 21 (1980) 1355–1356.
[16] J. Yamahara, H. Matsuda, H. Watanabe, Biologically active principles of crude drugs. Analgesic and anti-inflammatory effects of "Keigai(ShoyakugakuZasshi)", Yakugaku Zasshi 100 (1964) 33.
[17] C.A. Lipinski, F. Lombardo, B.W. Dominy, Experimental and computational approaches to estimate solubility and permeability in drug discovery and development settings, Adv. Drug Deliv. Rev. 46 (2001) 3–26.
[18] Y. Ikeda, D.M. Long, The molecular basis of brain injury and brain edema: the role of oxygen free radicals, Neurosurgery 27 (1990) 1–11.
[19] J.M. McCall, J.M. Braughler, E.D. Hall, Lipid peroxidation and the role of oxygen radicals in CNS injury, Acta Anaesthesiol. Belg. 38 (1987) 279–373.
[20] M. Guo, *Drosophila* as a model to study mitochondrial dysfunction in Parkinson's disease, Cold Spring Harb. Perspect. Med. 2 (2012) 11.
[21] M. Vila, S. Przedborski, Targeting programmed cell death in neurodegenerative diseases, Nat. Rev. Neurosci. 4 (2003) 365–375.
[22] C. Borner, The Bcl-2 protein family: sensors and check-points for life-or-death decisions, Mol. Immunol. 39 (2003) 615–647.
[23] A.M. Chinnaiyan, K. Orth, K. O'Rourke, Molecular ordering of the cell death pathway. Bcl-2 and Bcl-xL function upstream of CED-3-like apoptotic proteases, J. Biol. Chem. 271 (1996) 4573–4576.
[24] J. Kuroda, T. Ago, S. Matsushima, P. Zhai, M.D. Schneider, J. Sadoshima, NADPH oxidase 4 (Nox4) is a major source of oxidative stress in the failing heart, Proc. Natl. Acad. Sci. U. S. A. 107 (2010) 15565–15570.
[25] X.H. Liu, L.L. Pan, Q.H. Gong, Y.Z. Zhu, Antiapoptotic effect of novel compound from Herba leonuri — leonurine (SCM-198): a mechanism through inhibition of mitochondria dysfunction in H9c2 cells, Curr. Pharm. Biotechnol. 11 (2010) 895–905.
[26] B. Liu, Z. Jian, Q. Li, K. Li, Z. Wang, L. Liu, L. Tang, X. Yi, H. Wang, C. Li, T. Gao, Baicalein protects Human melanocytes from $H_{(2)}O_{(2)}$-induced apoptosis via inhibiting mitochondria-dependent caspase activation and the p38 MAPK pathway, Free Radic. Biol. Med. 53 (2012) 183–193.
[27] Y. Kitamura, T. Ota, Y. Matsuoka, I. Tooyama, H. Kimura, S. Shimohama, Y. Nomura, P.J. Gebicke-Haerter, T. Taniguchi, Hydrogen peroxide-induced apoptosis mediated by p53 protein in glial cells, Glia 25 (1999) 154–164.
[28] E.K. Kim, E.J. Choi, Pathological roles of MAPK signaling pathways in human diseases, Biochim. Biophys. Acta 1802 (2010) 396–405.

[29] Z.L. Que, W.J. Zhou, J. Chang, Neuroprotective effects of mercaptoethylleonurine and mercaptoethylguanidine analogs on hydrogen peroxide-induced apoptosis in human neuronal SH-SY5Y cells, Bioorg. Med. Chem. Lett. 23 (2013) 1793–1796.
[30] T.F. Franke, D.R. Kaplan, L.C. Cantley, PI3K: downstream AKTion blocks apoptosis, Cell 88 (1997) 435–437.
[31] M.H. Cardone, N. Roy, H.R. Stennicke, Regulation of cell death protease caspase-9 by phosphorylation, Science 282 (1998) 1318–1321.
[32] P.P. Roux, J. Blenis, ERK and p38 MAPK-activated protein kinases: a family of protein kinases with diverse biological functions, Microbiol. Mol. Biol. Rev. 68 (2004) 320–344.
[33] J. Liu, A. Lin, Role of JNK activation in apoptosis: a double-edged sword, Cell Res. 15 (2005) 36–42.
[34] Surojit Paul, John A. Connor, NR2B-NMDA receptor-mediated increases in intracellular Ca^{2+} concentration regulate the tyrosine phosphatase, STEP, and ERK MAP kinase signalling, J. Neurochem. 114 (2010) 1107–1118.
[35] J. Naarala, P. Tervo, J. Loikkanen, Blocking of carbachol-induced calcium mobilization by glutamate receptor antagonists, Neurosci. Res. Commun. 30 (2006) 1–6.
[36] R.S. Akundi, M. Hüll, H.W. Clement, 1-Trichloromethy 1,2,3,4-tetrahydro-β-carboline (TaClo) induces apoptosis in human neuroblastoma cell lines, Ann N Y Acad Sci 1010 (2003) 304–306.
[37] F. Zhou, Y. Xu, X.Y. Hou, MLK3-MKK316-P38MAPK cascades following N-methyl-D-aspartate receptor contributes to amyloid-β-peptide induced apoptosis in SH-SY5Y cells, J. Neurosci. Res. 92 (2014) 808–817.
[38] D. Petroni, J. Tsai, D. Mondal, Attenuation of low dose methylmercury and glutamate induced-cytotoxicity and tau phosphorylation by an N-methyl-D-aspartate receptor antagonist in human neuroblastoma (SH-SY5Y) cells, Environ. Toxicol. 28 (12) (2013) 700–706.
[39] M.V. Avshalumov, M.E. Rice, NMDA receptor activation mediates hydrogen peroxide-induced pathophysiology in rat hippocampal slices, J. Neurophysiol. 87 (2002) 2896–2903.
[40] T.I. Peng, J.T. Greenamyre, Privileged access to mitochondria of calcium influx through N-methyl-D-aspartate receptors, Mol. Pharmacol. 53 (1998) 974–980.
[41] Phillip H. Beske, Darrell A. Jackson, NADPH oxidase mediates the oxygen–glucose deprivation/reperfusion-induced increase in the tyrosine phosphorylation of the N-methyl-D-aspartate receptor NR2A subunit in retinoic acid differentiated SH-SY5Y cells, J. Mol. Signal. 7 (2012) 15.